Sharp magnetization steps induced by A-site substitution in $Pr_{0.5}Ca_{0.5}MnO_3$

2003 J. Phys.: Condens. Matter 15 7055

(http://iopscience.iop.org/0953-8984/15/41/013)

INSTITUTE OF PHYSICS PUBLISHING JOURNAL OF PHYSICS: CONDENSED MATTER

J. Phys.: Condens. Matter **15** (2003) 7055–7062 PII: S0953-8984(03)64520-0

Sharp magnetization steps induced by A-site substitution in $Pr_{0.5}Ca_{0.5}MnO_3$

B Raveau, D Zhu, A Maignan, M Hervieu, C Martin, V Hardy and S Hébert

Laboratoire CRISMAT, UMR 6508CNRS ENSICAEN,
6 boulevard Maréchal Juin, 14050 CAEN Cedex 4, France

Received 10 June 2003
Published 3 October 2003
Online at stacks.iop.org/JPhysCM/15/7055

Abstract

The possibility of inducing ferromagnetism by applying a magnetic field to a charge ordered CE-type antiferromagnet by means of calcium-site doping has been studied. It is shown that barium doping induces only very small ferromagnetic fractions in the absence of a magnetic field (<2%), but in contrast considerably lowers the critical field for the appearance of ferromagnetism (5 T instead of the 25 T for the pristine phase). Moreover, sharp magnetization steps are obtained by applying a magnetic field, a complete ferromagnetic state being reached for 8% Ba, under 5 T. Local structural distortions induced by barium may be responsible for the weakening of the orbital charge ordering.

The mechanism of the transition of $Ln_{1/2}Ca_{1/2}MnO_3$ manganites from an antiferromagnetic insulating (AFMI) to a ferromagnetic metallic (FMM) state when subjected to an external magnetic field is of great interest, in relation to understanding the colossal magnetoresistance (CMR) effect. In the absence of a magnetic field, these materials exhibit orbital and charge ordering in the form of 'Mn^{3+}' and 'Mn^{4+}' stripes alternating along one direction and are CE-type antiferromagnetic insulators [1–6]. It has been shown that by applying a high magnetic field, the charge ordered state can be collapsed, leading to the FMM state, as for instance in $Pr_{0.5}Ca_{0.5}MnO_3$ subjected to fields larger than 25 T at 1.4 K [7]. In order to lower the critical magnetic field required to reach the FMM state in these oxides, a first route was recently investigated which consists in doping Mn sites with various cations (see for a review [8]). The latter induce a disordering of the manganese orbitals and charges, so the CE-type AFM state is considerably weakened. As a result, doping with magnetic cations such as Cr, Co, Ni, Ru, Rh, Ir not only destroys the orbital charge ordering, but also induces a FMM state even in the absence of a magnetic field (see for instance [9–14]). In another way, non-magnetic d^0 and d^{10} cations such as Sc, Al, Ga, In, Sn, Ti, Mg considerably weaken charge ordering, with the result that the AFMI state becomes metastable, a spin glass-like behaviour being obtained in the absence of a field [15]. More importantly, these doped manganites exhibit

either a FMM state or a FM component when subjected to a small field (i.e. 5 T instead of 25 T). Most often, these Mn-site substituted manganites exhibit a phase separated ground state, in which short range ordered ferromagnetic and antiferromagnetic domains coexist. This phenomenon of phase separation is known to lie at the origin of many unusual features—for instance, the persistent memory effects reported in Fe doped $La_{0.5}Ca_{0.5}MnO_3$ [16]. Another striking behaviour was recently discovered in Mn-site doped $Pr_{0.5}Ca_{0.5}MnO_3$: at low enough temperatures ($T \sim 2$ K), one observes that the magnetization increases in the form of sharp steps, when increasing the applied field, suggesting that the ferromagnetism grows through a martensitic mechanism [17–19].

At this stage of the investigations, it appears that any event which locally disturbs the orbital ordering in $Ln_{0.5}Ca_{0.5}MnO_3$ should also weaken the charge ordering and consequently should induce similar magnetization steps on applying a magnetic field. In this respect, doping of the calcium sites with bigger cations such as barium is of interest, since it may introduce locally a structural distortion able to affect the orbital ordering. In this paper, we show that barium for calcium substitution in the manganite $Pr_{0.5}Ca_{0.5}MnO_3$ considerably lowers the critical field for the appearance of ferromagnetism. We observe that in these oxides $Pr_{0.5}Ca_{0.5-x}Ba_xMnO_3$ ($x < 0.1$), sharp magnetization steps are induced by applying a magnetic field, a complete ferromagnetic state being reached under 5 T (to be compared to 25 T for the pristine phase) by doping with barium.

The samples of the series $Pr_{0.5}Ca_{0.5-x}Ba_xMnO_3$ were prepared by conventional solid state reaction starting from intimate stoichiometric mixtures of Pr_6O_{11}, CaO, $BaCO_3$ and MnO_2 first heated at 1000 °C for 10 h to allow decarbonation and then pressed into the form of bars. The bars were then heated in air at 1200 °C for 12 h, sintered at 1500 °C for 12 h and then cooled at 5 °C min^{-1} down to 800 °C and finally quenched at room temperature. Energy dispersive spectroscopic (EDS) analysis shows that the cationic composition is identical to the nominal one. This confirms that barium has entered into the matrix and, due to its large size, sits in the A sites of the perovskite structure.

In phase separated systems, the grain size is a parameter which can affect the fractions of the different phases. The average grain size of the ceramic samples used in the present study is $\sim$10 μm for all compositions. According to the literature [20], such a grain size can be considered to be large enough to reflect the bulk properties and to allow field- and temperature-induced evolution of the phase separation.

The physical properties have been checked by means of dc magnetization (M), four-probe resistivity (ρ) and ac magnetic susceptibility (χ'). M measurements were carried out with a dc SQUID magnetometer (0–5.5 T), an ac–dc SQUID magnetometer (0–5 T) and a magnetic option (extraction method) of a Physical Properties Measurement System (PPMS) (0–9 T), respectively. The PPMS was also used to measure ρ and ac $\chi(T)$. All the systems are from Quantum Design Company. Because the physical properties of these samples are history dependent, virgin pieces of the samples were used for each measurement. The samples were zero-field cooled from room temperature down to the measuring temperature with temperature sweep rates of 10–20 K min^{-1} before the measurements of the magnetic field-dependent M and ρ. The magnetic field was swept at 0.025 T s^{-1} and there was a pause of 30 s prior to M data collection. The ac $\chi(T)$ measurements were performed under an excitation field and a frequency of 10 Oe and 10^4 Hz respectively.

The magnetization curves $M(H)$ registered at 2.5 K show that Ba doped manganites (figure 1) exhibit sharp magnetization steps when subjected to an external magnetic field, in contrast to the undoped phase, $Pr_{0.5}Ca_{0.5}MnO_3$, for which no such abrupt jumps of magnetization are detected up to 25 T [7]. This behaviour is very similar to that observed for Mn-site doped, $Pr_{0.5}Ca_{0.5}Mn_{1-x}M_xO_3$ manganites [17–19].

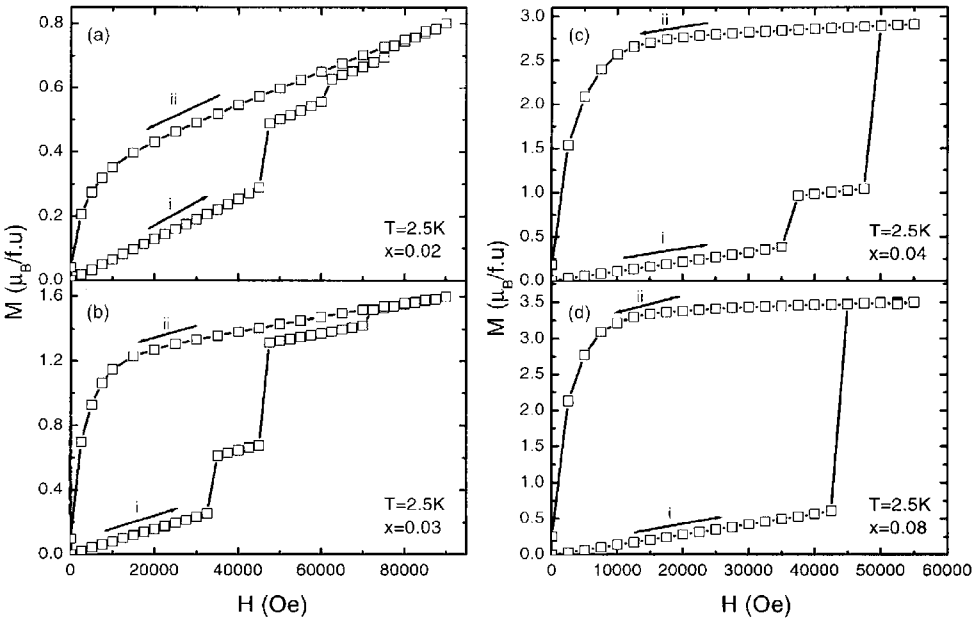

Figure 1. Magnetic field dependences ((i) increasing and (ii) decreasing the field) of the isothermal ($T = 2.5$ K) magnetization for the $Pr_{0.5}Ca_{0.5-x}Ba_xMnO_3$ compounds. (a) $x = 0.02$, (b) $x = 0.03$, (c) $x = 0.04$, (d) $x = 0.08$.

Remarkably high magnetization values are reached for the barium substituted oxides, $Pr_{0.5}Ca_{0.5-x}Ba_xMnO_3$, as exemplified by the $x = 0.08$ sample (figure 1(d)) for which a magnetic moment of 3.5 μ_B, i.e. close to the theoretical value, is achieved at 2.5–5 K, under 5 T. This value is close or even superior to the largest magnetic moments $M_{5\,T}$ obtained for the manganites doped with non-magnetic cations at the Mn site which range from 2.6 μ_B (for Ga doping) to 3.0 μ_B (for Sn doping) at 5 K [21]. Like for the latter, the transition is irreversible, the higher magnetization values being reached on the decreasing branch of the magnetization half-loop curve ((ii) decreasing field) registered at 2.5 K. The larger M values induced by the magnetic field of the A-site substituted manganites compared to B-site ones are consistent with the magnetic dilution effect created by the diamagnetic cations substituted for Mn in the latter. An interesting feature relates to the regular increase of the maximum value of the magnetization induced by the largest magnetic fields with the barium content: for example, under 5 T the magnetization increases from 0.5 μ_B for $x = 0.02$ (figure 1(a)) to 1.3 μ_B for $x = 0.03$ (figure 1(b)), then to 2.9 μ_B for $x = 0.04$ (figure 1(c)) and finally reaches 3.5 μ_B for $x = 0.08$ (figure 1(d)). In contrast, the dM/dH slope on the virgin M curve, before the first magnetization step, is only slightly changing with x, as shown in figure 1. It must be pointed out that this ability of barium to facilitate the field-induced ferromagnetism decreases abruptly beyond $x = 0.09$, i.e. for $x = 0.10$–0.15, since maximum $M_{5\,T}$ values of 0.6 μ_B can only be obtained at 2.5 K.

Table 1 clearly shows that M reaches almost the theoretical saturation (3.5 $\mu_B\,fu^{-1}$ without taking into account the Pr^{3+} contribution) for compositions in the range $x = 0.06$–0.08, for applied field values H_{max} ranging from 4.5 to 5.5 T. From this table we can also observe that the number of steps taken to reach the maximum value of the magnetic moment M_{max} at 2.5 K decreases as x increases and correspondingly the applied magnetic field required to reach M_{max} decreases. For $x = 0.02$ and 0.03 we do indeed observe that the saturation is far

Table 1. The ferromagnetic (FM) fraction under 0.25 T, magnetization under 5 T on the increasing branch ($M_{5\,\mathrm{T}}$), maximum magnetization M_{max} in either 5 or 5.5 or 9 T ($=H_{max}$), number of steps, height of the first step (ΔM_1) and value of the 'critical' field (H_c) measured at 2.5 K for $Pr_{0.5}Ca_{0.5-x}Ba_xMnO_3$ manganites.

x	FM fraction (%)	$M_{5\,\mathrm{T}}$ (μ_B fu^{-1})	M_{max} (μ_B)	H_{max} (T)	Number of steps	1st step height ΔM_1 (μ_B)	H_{c_1} (T)	H_{c_2} (T)	H_{c_3} (T)	2nd step ΔM_2 (μ_B)
0.02	0.8	0.5	0.8	9	3	0.2	4.5	6.0	7.5	0.1
0.03	0.9	1.3	1.6	9	3	0.4	3.3	4.5	7.0	0.6
0.04	1.3	2.9	2.9	5.5	2	0.6	3.5	4.8		1.9
0.05	1.5	2.7	2.7	5	1	2.1	4.0			
0.06	1.4	3.3	3.3	5.5	1	2.6	4.8			
0.07	1.6	3.4	3.4	5.5	1	2.5	5.3			
0.08	1.5	3.5	3.5	5.5	1	2.9	4.3			
0.09	1.5	0.7	0.8	5.5	No	No	No	No	No	No
0.10	1.4	0.6	0.6	5	No	No	No	No	No	No
0.15	1.3	0.6	0.6	5	No	No	No	No	No	No

from being achieved ($M_{max} \sim 0.8\ \mu_B$ and $\sim 1.6\ \mu_B$, respectively, in 9 T), whereas three steps are necessary to reach these M_{max} values (figures 1(a), (b)). For $x = 0.04$, only two steps are necessary to reach M_{max} in a much lower field (5 T) (figure 1(c)), whereas the saturation ($M_{max} \sim 3.5\ \mu_B$) is finally reached for $x = 0.08$ in only one step and with a field of only 4.5 T (figure 1(d)). In contrast, the value of the critical field for the appearance of the first step does not vary regularly, ranging from 3.3 to 5.3 T in the range $x = 0.02$–0.08. The height of the successive steps for low x values also varies in an irregular way: for $x = 0.02$ the second step is smaller than the first one, whereas for $x = 0.03$ and 0.04, the opposite is observed. Finally it must be emphasized that the ferromagnetic fraction at 2.5 K, obtained from the magnetic measurements under 0.25 T, is very small, ranging from 0.8% to 1.6%, showing again a similar behaviour to the manganites $Pr_{0.5}Ca_{0.5}Mn_{1-x}M_xO_3$ doped with non-magnetic cations (M = Ga, Al, Sn, Ti, Sc, Mg, ... [21]).

The evolution of the resistivity versus the applied field, registered at 2.5 K (figure 2), also shows a step-like behaviour. For $x = 0.02$, no observation can be made, due to the too highly insulating character of the sample ($\rho > 10^7\ \Omega$ cm even in 7 T). For $x = 0.03$, two sharp drops of the resistivity at 4.8 and 7 T are observed (figure 2(a)) corresponding to the second and third magnetization steps respectively (figure 1(b)). The too high resistivity of the sample below 4 T prevents the first step from being observed. Note that in the second step the resistivity decreases by more than two orders of magnitude. For $x = 0.04$, the step around 3.5 T cannot be seen due to the too high resistivity of the sample, whereas one step is observed around 4.5 T (figure 2(b)) in agreement with the $M(H)$ measurements (figure 1(c)); moreover one additional step appears around 6.2 T which was not measured in the $M(H)$ curve that stopped at 5.5 T. Finally for $x = 0.08$ one step is observed around 4.5 T (figure 2(c)) in agreement with the $M(H)$ loop (figure 1(d)) and a second step appears around 6.8 T, which was not measured in $M(H)$ which was only recorded up to 5.5 T.

In order to understand the peculiar effect of Ba doping upon the magnetic and transport properties of the $Pr_{0.5}Ca_{0.5-x}Ba_xMnO_3$ series, ac susceptibility measurements (without an applied dc magnetic field) were carried out while cooling from 350 down to 5 K. The $\chi'(T)$ curves (figure 3) show that the bump at 250 K, characteristic of orbital charge ordering in the undoped phase $Pr_{0.5}Ca_{0.5}MnO_3$, is slightly shifted towards a lower temperature (230 K) and flattened for the $x = 0.02$ sample and this effect is even more pronounced for the $x = 0.04$

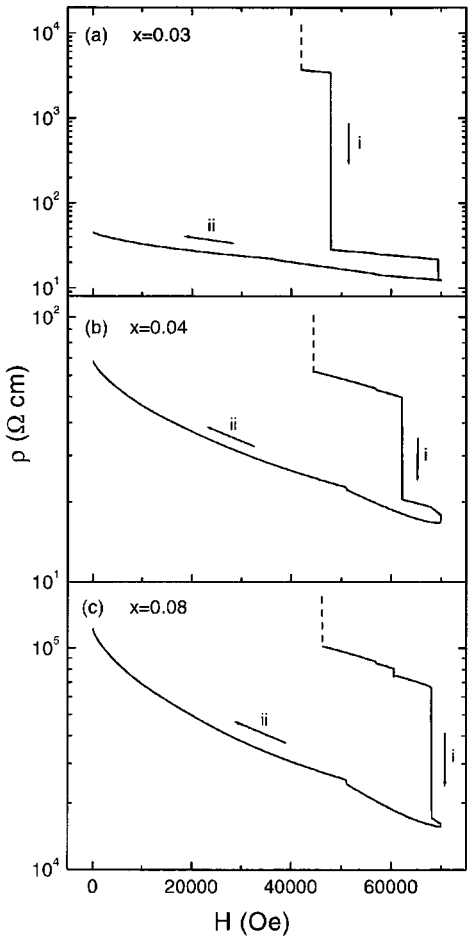

Figure 2. The evolution of the resistivity versus the applied field ((i) increasing and (ii) decreasing the field) registered at 2.5 K for $Pr_{0.5}Ca_{0.5-x}Ba_xMnO_3$. (a) $x = 0.03$, (b) $x = 0.04$, (c) $x = 0.08$.

sample. Furthermore, for these two phases, a new bump at about 140 K is also observed. For higher Ba contents, e.g. $x \geqslant 0.05$, the bump around ∼200–220 K still exists and a cusp appears around 50 K (figure 3; e.g. $x = 0.08$). The latter is significantly shifted on changing the frequency (inset of figure 3; $x = 0.10$), so it can be considered that a spin glass-like behaviour is then induced by Ba doping. Note that the peak around 50 K is accompanied by a smaller peak at 40 K; such a behaviour could originate from the presence of a small amount of Mn_3O_4. The origin of the faster decrease of χ below 140 K is probably the appearance of an antiferromagnetic state. A neutron diffraction study will be necessary to understand these behaviours.

The electron diffraction (ED) study of the $x = 0.05$ and 0.1 samples was carried out by reconstructing the reciprocal space of more than 50 crystals, also systematically analysed by energy dispersive spectroscopy (EDS). All the crystallites of the $x = 0.05$ and 0.1 samples exhibit at room temperature a *Pnma*-type structure ($a_p\sqrt{2}$, $2a_p$, $a_p\sqrt{2}$) similar to that of the undoped compound. The EDS analyses attest to the homogeneity of both samples, with actual cationic compositions in agreement with the nominal ones.

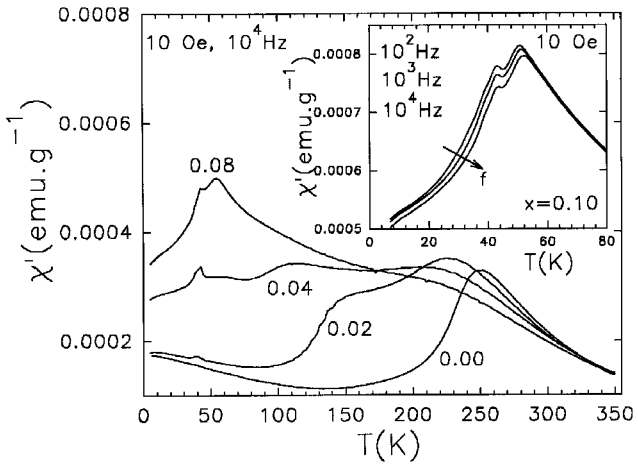

Figure 3. The real part of the magnetic susceptibility (χ') as a function of temperature for the $Pr_{0.5}Ca_{0.5-x}Ba_xMnO_3$ samples (x values are labelled on the graph). Inset: the frequency dependence of $\chi'(T)$ in the low temperature region for $x = 0.10$.

The microstructural characterization of $Pr_{0.5}Ca_{0.45}Ba_{0.05}MnO_3$ was carried out with a TOPCON 002B microscope (200 and $C_s = 0.4$ mm), using bright field (BF)/dark field (DF) and high resolution electron microscope (HREM) techniques (figures 4(a), (b)). Depending on the focus value, the HREM images exhibit more or less visible local deviations of the contrast with respect to the evenness expected for perfect crystal structure (see for example the [010] image in figure 4(b)). Theoretical calculations show that the key parameter is the position of the oxygen atoms, the difference in scattering factors values of the A cations being negligible in comparison. Such an effect can be understood considering the large size of one Ba^{2+} cation with respect to that of Pr^{3+}–Ca^{2+}. The substitution mechanism would necessarily involve a local displacement of the surrounding atoms, especially the bridging oxygens. Working with BF/DF imaging provides microstructural information. The local distortions induce strain effects at a larger scale, clearly observed in the dark field images, as shown by the highly disturbed contrast in figure 4(a). The strain effects increase with x, so for $x = 0.1$, the ED spots exhibit weak and diffuse arms elongated along [100]* and [001]*.

At 92 K, i.e. below T_{CO}, the $Pr_{0.5}Ca_{0.45}Ba_{0.05}MnO_3$ crystallites exhibit a system of additional reflections (see the white arrows in figure 4(c)), characteristic of the 'CO' phenomena. The modulation vector is $q\boldsymbol{a}^*$, with q equal or approximately equal to $1/2$, in agreement with mixed valence of Mn ($Mn^{3+} = Mn^{4+}$).

At this point of the investigation, a martensitic-like scenario, based on the strain accommodation in phase separated manganites [18, 19, 22], can be proposed to explain the similarity of the Ba- and Mn-site substitution effects, both leading to sharp magnetization steps at low T in the $Pr_{0.5}Ca_{0.5}MnO_3$ manganite. The substitution of barium for calcium locally distorts the structure, due to the size difference between calcium and barium. Consequently this effect tends to weaken the orbital and charge ordering. This effect may be responsible for the appearance of the spin glass-like behaviour observed in the $\chi'(T)$ curves. Under application of an external magnetic field, these disordered spins align more easily to reach the FM state compared to the robust CE-type AFM of $Pr_{0.5}Ca_{0.5}MnO_3$, leading to a large M value of $\sim$3.5 μ_B in only 5.5 T for an optimal value of the barium concentration ($x = 0.06$–0.08).

Then, the appearance of sharp magnetization steps in the Ba doped manganites can also be explained by the martensitic scenario: the magnetic field application favours the development

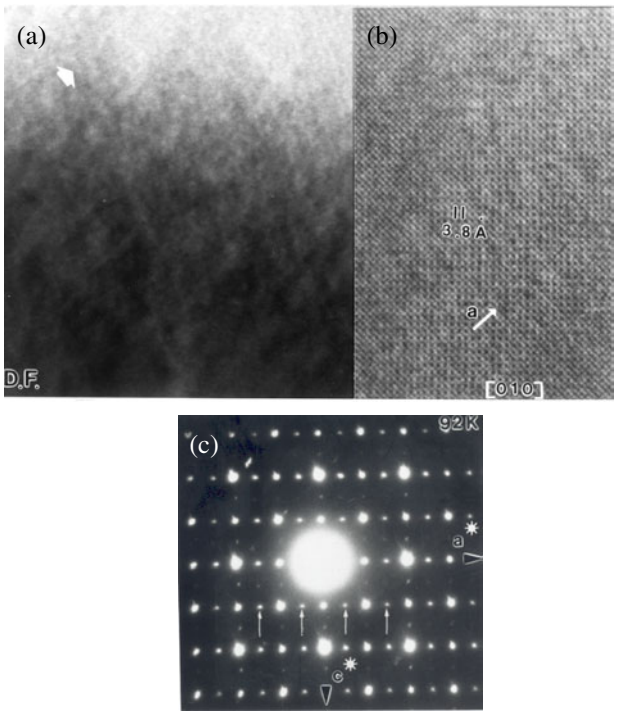

Figure 4. (a) Dark field (DF) and (b) [010] high resolution electron microscopy images recorded at room temperature. (c) An [010] ED pattern recorded at 92 K. The extra reflections, indicated by white arrows, are the signature of CO. They are observed along $\boldsymbol{a}^*$, involving a doubling of the parameter (note that a second set of weaker spots is observed in the perpendicular direction, due to the usual presence of twinning domains).

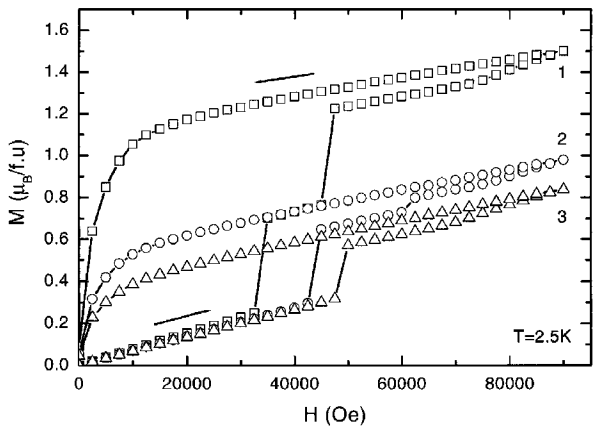

Figure 5. Successive isothermal ($T = 2.5$ K) $M(H)$ half-loops for $Pr_{0.5}Ca_{0.47}Ba_{0.03}MnO_3$. Between successive measurements, the sample is warmed up to 300 K and then zero-field cooled to 2.5 K.

of ferromagnetic regions around each barium impurity. The latter FM regions have a different symmetry as compared to the CO AFM matrix, resulting in elastic constraints at the interface between the FM region and AFM matrix. As the magnetic field increases, the magnetic energy

favours the FM development, but the latter is unfavourable from the elastic energy point of view. Thus, the FM regions cannot grow continuously and, finally, for a sufficient magnetic field, i.e. magnetic energy, the elastic constraints can be overcome as previously described for Mn-site doped manganites [18] leading to an M jump. The effect of thermal cycling upon $M(H)$ also supports this martensitic-like mechanism. As exemplified for $x = 0.03$ (figure 5), one does indeed observe that the value of the magnetization maximum decreases and the value of the critical magnetic field H_{c_1} for the appearance of the first step increases as the number of cycles increases, a phenomenon previously observed for Mn-site doped manganites [17–19, 21, 23].

In conclusion, the large A-site cationic size difference seems thus to provide an efficient way to generate sharp magnetization steps in an AF matrix. Further studies are now in progress to elucidate the exact role of the A-site cationic size in the magnetic ground state.

References

[1] Jirak Z, Krupicka S, Simsa Z, Dlouha M and Vratislav S 1985 *J. Magn. Magn. Mater.* **53** 153
[2] Chen C H and Cheong S W 1996 *Phys. Rev. Lett.* **76** 4042
[3] Radaelli P G, Cox D E, Marezio M and Cheong S W 1997 *Phys. Rev.* B **55** 3015
[4] Hervieu M, Barnabé A, Martin C, Maignan A, Damay F and Raveau B 1999 *Eur. Phys. J.* B **8** 31
[5] Woodward P M, Cox D E, Vogt T, Rao C N R and Cheetham A K 1999 *Chem. Mater.* **11** 3528
[6] Damay F, Jirak Z, Martin C, Maignan A, Raveau B, André G and Bourée F 1998 *J. Magn. Magn. Mater.* **190** 221
[7] Tokunaga M, Miura N, Tomioka Y and Tokura Y 1998 *Phys. Rev.* B **57** 5259
[8] Raveau B, Hervieu M, Maignan A and Martin C 2001 *J. Mater. Chem.* **11** 29
[9] Raveau B, Maignan A, Martin C and Hervieu M 1997 *J. Solid State Chem.* **130** 162
Raveau B, Maignan A, Martin C and Hervieu M 1997 *Mater. Res. Bull.* **32** 965
[10] Vanitha P V, Arulraj A, Raju A R and Rao C N R 1999 *C. R. Acad. Sci.* **2** 595
[11] Katsufuji T, Cheong S W, Mori S and Chen C H 1999 *J. Phys. Soc. Japan* **68** 1090
[12] Martin C, Maignan A, Hervieu M, Autret C, Raveau B and Khomskii D I 2001 *Phys. Rev.* B **63** 174402
[13] Kimura T, Tomioka Y, Kumai R, Okimoto Y and Tokura Y 1999 *Phys. Rev.* B **83** 3940
[14] Hébert S, Maignan A, Frésard R, Hervieu M, Retoux R, Martin C and Raveau B 2001 *Eur. Phys. J.* B **24** 85
[15] Hébert S, Maignan A, Martin C and Raveau B 2002 *Solid State Commun.* **121** 229
[16] Levy P, Parisi F, Granja L, Indelicato E and Polla G 2002 *Phys. Rev. Lett.* **89** 137001
[17] Hébert S, Hardy V, Maignan A, Mahendiran R, Hervieu M, Martin C and Raveau B 2002 *J. Solid State Chem.* **165** 6
[18] Hardy V, Hébert S, Maignan A, Martin C, Hervieu M and Raveau B 2003 *J. Magn. Magn. Mater.* **264** 183
[19] Hébert S, Maignan A, Hardy V, Martin C, Hervieu M, Raveau B, Mahendiran R and Schiffer P 2002 *Eur. Phys. J.* B **29** 419
[20] Levy P, Parisi F, Polla G, Vega D, Leyva G and Lanza H 2000 *Phys. Rev.* B **62** 6437
[21] Hébert S, Maignan A, Hardy V, Martin C, Hervieu M and Raveau B 2002 *Solid State Commun.* **122** 335
[22] Podzorov V, Kim B G, Kiryukhin V, Gershenson M E and Cheong S W 2001 *Phys. Rev.* B **64** 140406
[23] Mahendiran R, Maignan A, Hébert S, Martin C, Hervieu M, Raveau B, Mitchell J F and Schiffer P 2002 *Phys. Rev. Lett.* **89** 286602